IIETA International Information and Engineering Technology Association
Advancing the World of Information and Engineering

Journal of New Materials for Electrochemical Systems
Vol.23, No.2, April, 2020, pp. 61-65
http://new-mat.org
http://iieta.org/journals/jnmes

Influence of Calcination Temperature on the Electrochemical Performance of $Li_{1.2}[Ni_{0.13}Co_{0.13}Mn_{0.54}]_{0.985}Zr_{0.015}O_2$ as Li-rich Cathode Material for Li-ion Batteries

Milad Ghorbanzadeh[1], E. Allahyari[2], R. Riahifar[1*], S.M.M. Hadavi[3]

[1] Battery and Sensor Group, Materials and Energy Research Center, Karaj, Iran
[2] Materials Science and Engineering Department, Iran University of Science and Engineering, Tehran, Iran
[3] Department of Materials Engineering, University of Tarbiat Modares, Tehran, Iran

Corresponding Author Email: reza_rfr@yahoo.com

ABSTRACT

In this work, $Li_{1.2}[Ni_{0.13}Co_{0.13}Mn_{0.54}]_{0.985}Zr_{0.015}O_2$ cathode material was synthesized via combustion synthesis method. The product was annealed at different temperatures of 650, 750 and 850 °C for 12 h. The effect of annealing temperature on electrochemical performance of synthesized powder was investigated using charge/discharge performance, cyclic voltammetry and impedance tests. X-ray diffraction (XRD) analysis and scanning electron microscopy (SEM) were used for phase identification and investigating the morphology of the samples. According to charge/discharge diagrams, the sample calcined at 750 °C exhibited the highest initial discharge capacity of 254 mAh/g at current density of 25 mA/g. The highest cyclic stability was obtained at 750 °C so that the remained capacity after 50 cycles was about 97%. Impedance tests and Nyquist diagrams revealed that the lowest impedance is observed at 750 °C.

Keywords: *combustion synthesis, Li-rich cathode material, calcination temperature, Li-batteries*

Received: December-17-2019, Accepted: March-03-2020, https://doi.org/10.14447/jnmes.v23i2.a01

1. INTRODUCTION

Ever-increasing advances in transportation has provided a great opportunity for developing battery cathode materials. Among different kinds of batteries, Li-ion batteries have gained a lot of interest due to high energy density and rather simple reactions. Relative slow progress of cathode materials has limited the development on Li-ion batteries. NCM cathode materials have been proposed as the main choice for cathode material in Li-ion batteries [1-4]. NCM Li-ion batteries offer high efficiency, high capacity, long life and better safety. In NCM batteries, $Li[Li_{0.2}\ Mn_{0.54}Ni_{0.13}Co_{0.13}]O2$ rich materials have been suggested as an efficient cathode material due to high capacity of about 250 mAh/g, low cost and lower pollution because of lower amount of cobalt content [5-8]. However, a major limitation of irreversible capacity loss has been observed for these batteries which is caused by extraction of lithium in the form of Li_2O at high potentials. In other words, the first charging cycle is accompanied by extraction of lithium as well as removal of oxygen vacancies at higher potentials leading to reduction of active sites for storage of Li^+ ions during subsequent cycles [9, 10]. Another result, the formation of SEI film reduces the Li^+ diffusion coefficient and electrical conductivity [5, 11, 12].

In recent years, several methods have been proposed in order to improve the electrochemical performance of Li-ion batteries including novel synthesis techniques [13-15], doping [16-22], surface coating [23-26] and using composite materials [27]. It has been shown that doping in cathode material structure is an efficient way to enhance cycle stability. By incorporation of the doping elements in the crystalline structure of the cathode material, lattice parameter is changed resulting in improvement of electrochemical performance of the material [28, 29]. Song et al. [18] reported that doping appropriate amount of Ru leads to increase of lattice parameter and volume which can result in better electrochemical performance by encouraging the diffusion of Li^+ ion and hence improvement. In this study, Zr was used as doping element and effects of different calcination temperatures on structure and electrochemical properties of Zr-doped cathode materials prepared by combustion synthesis method were investigated.

2. EXPERIMENTAL PROCEDURES

An aqueous solution containing stoichiometric amounts of metal nitrate and citric acid was prepared. Ratio of stoichiometric amounts of oxidizers and reducers equal unity which guaranties that maximum amount of heat is released during the reaction. Prepared solution was stirred for 6 hours at 80 °C. During stirring, the water content is gradually lost and a viscous concentrated solution is obtained. Then, stirring temperature was raised by 100 °C in order to remove the retained water content as well as water of crystallization of metal nitrates available in the viscous redox (reduction-oxidation) solution. In this situation, citric acid is melted and an opaque melt is obtained. By further heating, the melt start to foam and then combustion begins. During combustion stage, heater temperature was retained constant at 300 °C. Combustion occurs in a few seconds with a flame in the center of the dried gel releasing large amounts of gas. The whole process took 10 minutes. In order to determine optimized calcination temperature, specimens were heat treated for 12 hours at different temperatures of 650, 750 and 850 °C. Galvanostatic tests were performed in the voltage range of 2.5-4.5 V to evaluate the electrochemical properties of the samples. For this purpose, a handmade cell was prepared and the process was done in a glove box. In order to prepare the

electrode used in galvanostatic tests, 75 wt.% cathode powder, 10 wt.% black carbon as conducting material and 15 wt.% PVDF and NMP as binder were mixed in the form of a slurry. The obtained slurry was coated on an aluminum foil and it was dried for 4 hours at 50 °C. Coated aluminum foil was cut to desired dimensions in accordance with the test standard. Electrolyte used in electrochemical test contained $LiPF_6$ dissolved in ethylene carbonate and dimethyl carbonate. Impedance test were performed on an EG&G Instruments Princeton Applied Research1025Model.

Phase identification was done using X-ray diffraction (XRD) analysis by a Phillips multi-purpose diffract meter (MPD). Microscopic observations were made on a Phillips XL40 scanning electron microscope (SEM) in order to evaluate microstructure and morphology of the specimens.

3. RESULTS AND DISCUSSION

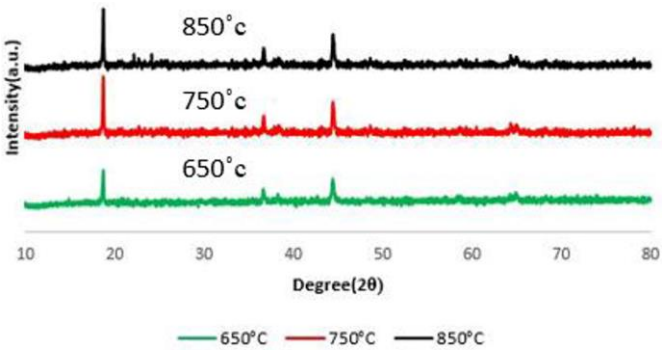

Figure 1. XRD patterns of $Li_{1.2}$ $[Ni_{0.13}Co_{0.13}$ $Mn_{0.54}]_{0.985}$ $Zr_{0.015}O_2$

X-ray diffraction (XRD) pattern obtained from different specimens are shown in Figure 1. According to this figure, all XRD patterns are related to α-$NaFeO_2$ with hexagonal structure and $R\bar{3}m$ symmetry. A lower peak intensity is observed for the specimen calcined at 650 °C which indicates that crystallization cannot be completed at this temperature. By raising the calcination temperature up to 750 °C, significant increase in peak intensity is observed which is due to further progress in crystallization.

It is generally certified that the value of c/a and peak intensity ratio of (003)/(104) indicate, respectively the layered structure and degree of cationic dimensional order [30-32].

It has been shown that when this ratio is lower than 1.2, Li^+ ions movements into and out of the crystal structure will be limited. Lattice parameters and $I_{(003)}/I_{(104)}$ for the specimens calcined at 650, 750 and 850 °C are summarized in Table 1. According to this table, the specimen calcined at 650 °C has the highest level of cation mixing due to its low $I_{(003)}/I_{(104)}$ ratio. In addition, the highest $I_{(003)}/I_{(104)}$ and *c/a* ratios are obtained by calcining at 750 °C. This is an indication of a layered structure which can inhibit movement of Li^+ in to and out of the crystal structure, hence improving the electrochemical properties of the cathode material especially initial discharging.

SEM micrographs showing the microstructure of different specimens are demonstrated in Figure 2. By calcining at 650 °C, no obvious change in particle size and morphology is observed revealing that particle growth does not occur at this temperature. On the other hand, a more uniform distribution of more spherical particles is obtained by calcining at 750 °C. By raising the calcination temperature to 850 °C, particles grow significantly and agglomeration takes place. In this case, effective surface is reduced leading to a hindrance in movement of Li^+ ions [33].

Table 1. Unit cell parameters of $Li_{1.2}$ $[Ni_{0.13}Co_{0.13}$ $Mn_{0.54}]_{0.985}$ $Zr_{0.015}O_2$ at different temperatures

Temperature	*a* (A^0)	*c* (A^0)	*c/a*	I(003)/I(104)
650^0c	2.8447	14.1807	4.9848	1.1027
750^0c	2.8490	14.21818	4.9905	1.4485
850^0c	2.8510	14.2265	4.9898	1.3421

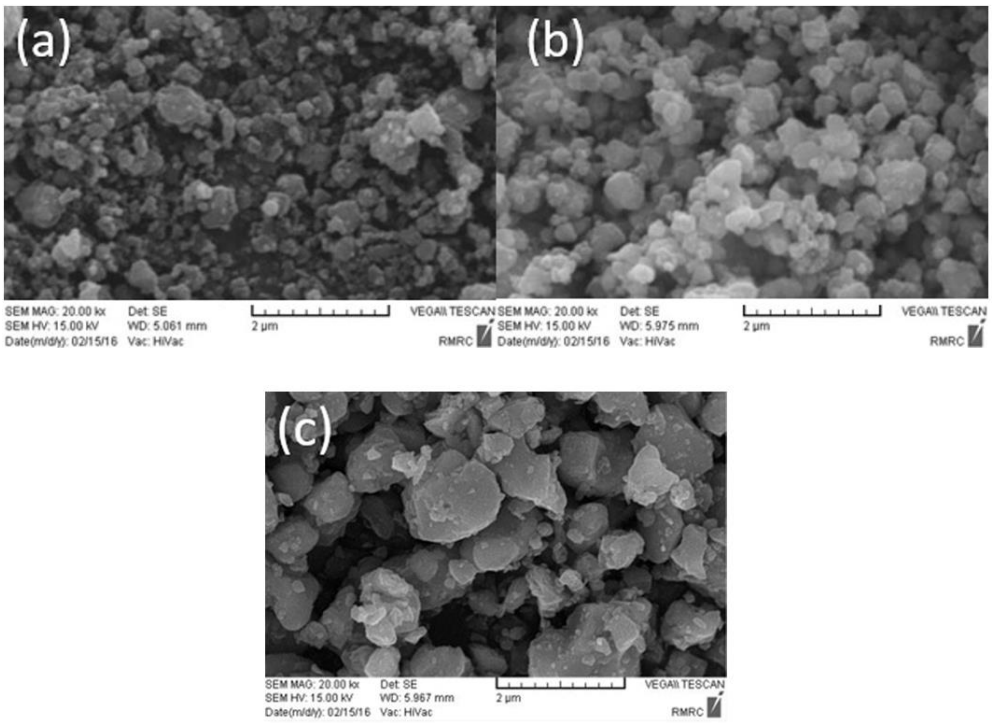

Figure 2. SEM photographs of $Li_{1.2}$ $[Ni_{0.13}Co_{0.13}$ $Mn_{0.54}]_{0.985}$ $Zr_{0.015}O_2$ at a)650°c b)750°c c)850° c

The EDS of sample is shown in Figure3 and confirm that the Zr elements are homogenously distributed in the samples.

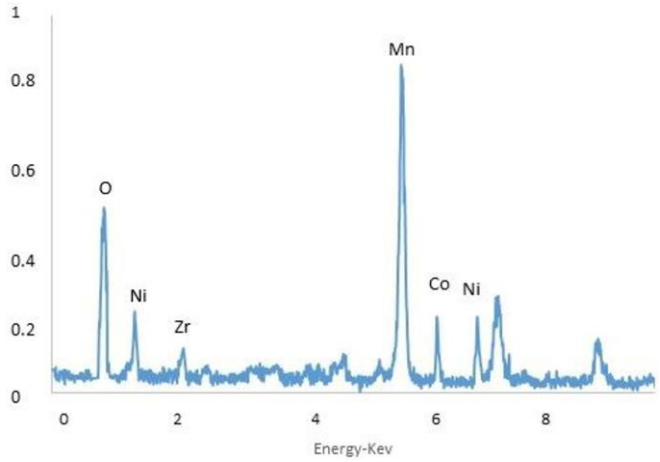

Figure 3. The EDS patterns of Zr substitution on $Li_{1.2}$ $[Ni_{0.13}Co_{0.13}Mn_{0.54}]O_2$

Figure 4 shows the initial charge/discharge capacity at the current intensity of 250 mAh/g for Zr-doped cathode materials calcined at different temperatures. It can be observed that the specimens calcined at 650, 750 and 850 °C exhibit initial discharge capacity of 239, 254 and 247 mAh/g, respectively, revealing that calcining at 750 °C yields the highest capacity.

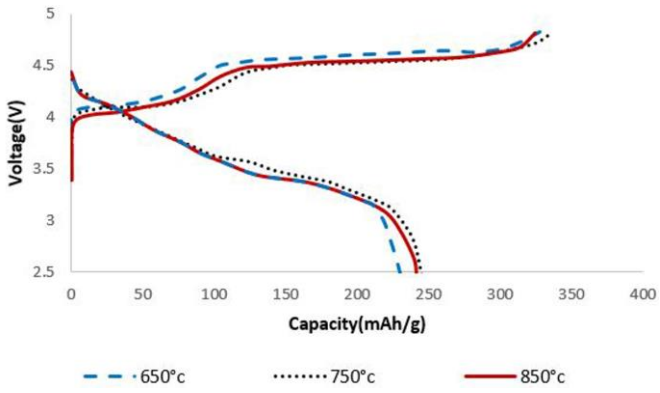

Figure 4. First charge–discharge curves of $Li_{1.2}$ $[Ni_{0.13}Co_{0.13}$ $Mn_{0.54}]_{0.985}$ $Zr_{0.015}O_2$ at different temperatures

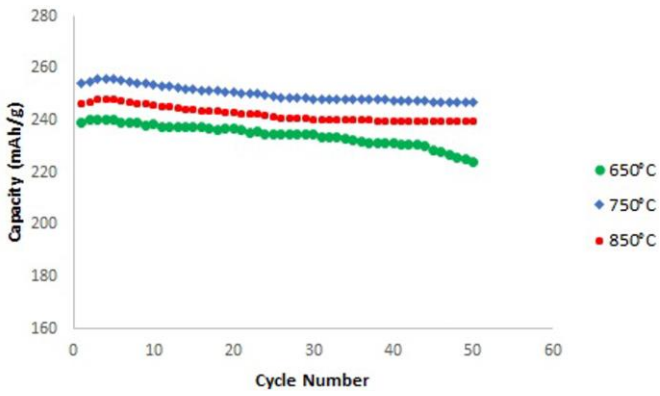

Figure 5. Cycling performance of $Li_{1.2}$ $[Ni_{0.13}Co_{0.13}$ $Mn_{0.54}]_{0.985}$ $Zr_{0.015}O_2$ at different temperatures

Evaluating the cyclic stability during the first 50 cycles (Figure 5) shows that the lowest capacity fade is observed for the specimen calcined at 750 °C. Better stability and higher amounts of remained capacity obtained for this specimen is related to high c/a ratio as well as more uniform morphology of the particles. Remained capacity for different specimens can be seen in Table 2.

Table 2. Charge/ discharge capacities of $Li_{1.2}$ $[Ni_{0.13}Co_{0.13}$ $Mn_{0.54}]_{0.985}$ $Zr_{0.015}O_2$ for initial and after 50 cycles at different temperatures

Sample	650°C	750°C	850°C
initial discharger specific capacity/ mAh g^{-1}	239	254	247
after 50 cycles/ mAh g^{-1}	223	247	238
capacity retention/%	93%	97%	96%

Cyclic voltammetry (CV) diagram measured for the specimen calcined at 750 °C is demonstrated in Figure 6. Based on this figure it can be stated that oxidation and reduction reactions corresponding to Ni^{2+}/Ni^{4+} [34] redox reaction occur at 3.78 V and 4.14 V, respectively. In addition, the 5th, 15th and 20th cycles of the doped specimen are very similar indicating the high reversibility and low polarization of the specimens.

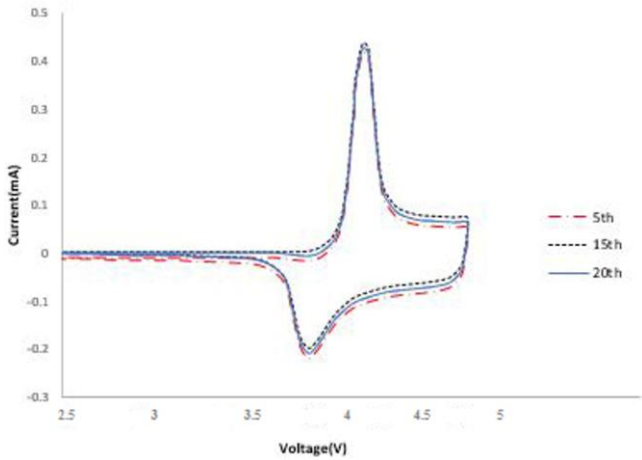

Figure 6. CV profiles of $Li_{1.2}$ $[Ni_{0.13}Co_{0.13}$ $Mn_{0.54}]_{0.985}$ $Zr_{0.015}O_2$ at 750°c

Two separate regions can be discerned in the Nyquist diagrams obtained for different temperatures (Figure 7). First region is a semicircle corresponding to S Evaluating the discharge capacity EI film ($R_f||C_{sl}$) at high frequencies and charge transfer phenomenon at medium to high frequencies ($R_{ct}||C_{dl}$). The second region is a line with a 45° angle to the real axis which is related to Warburg resistance (W). The latter region describes a frequency range at which reaction kinetics is limited by the rate of chemical diffusion reactions in the electrode. Using impedance tests, the reactions limiting the process rate through both charge transfer and mass transfer mechanisms can be determined precisely. Figure 7 reveals that the specimen calcined at 750 °C has the loest charge-transfer resistance. This is due to the fact that this specimen has a larger lattice parameter which facilitates the movement of Li^+ ions. On the other hand, the specimen calcined at 650 °C exhibits the highest electrochemical impedance which is related to more compact crystal structure of this specimen. The higher charge-transfer resistance of the specimen calcined at 850 °C is mainly attributed to the agglomeration of particles and more difficult diffusion of Li^+ ions.

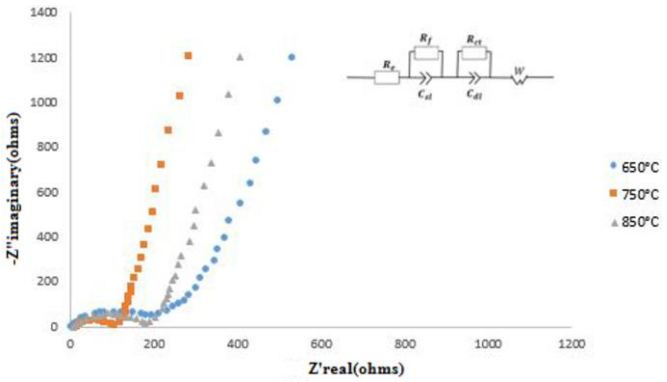

Figure 7. Nyquist plots of $Li_{1.2}$ $[Ni_{0.13}Co_{0.13}$ $Mn_{0.54}]_{0.985}$ $Zr_{0.015}O_2$ at different temperatures

4. CONCLUSIONS

$Li_{1.2}[Ni_{0.13}Co_{0.13}Mn_{0.54}]_{0.985}Zr_{0.015}$ cathode material was prepared via combustion synthesis method. SEM observations showed that particle size is increased by raising the calcination temperature from 650 to 850 °C. SEM and XRD results revealed that calcining at 750 °C yields larger lattice parameters and a more uniform microstructure compared to specimens calcined at other temperatures. Based on electrochemical tests, the specimen calcined at 750 °C exhibits the best electrochemical properties including high initial discharge capacity of 254 mAh/g and better stability during the first 50 cycles determined by the remained capacity of 97%. Cyclic voltammetry confirmed improved reversibility and reduction on concentration polarization of the specimen calcined at 750 °C.

REFERENCES

[1] Makimura, Y., Ohzuku, T. (2003). Lithium insertion material of LiNi1/2Mn1/2O2 for advanced lithium-ion batteries. Journal of Power Sources, 119: 156-160. https://doi.org/10.1016/S0378-7753(03)00170-8

[2] Lee, M.H., Kang, Y.J., Myung, S.T., Sun, Y.K. (2004). Synthetic optimization of Li [Ni1/3Co1/3Mn1/3] O2 via co-precipitation. Electrochimica Acta, 50(4): 939-948. https://doi.org/10.1016/j.electacta.2004.07.038

[3] Koyama, Y., Makimura, Y., Tanaka, I., Adachi, H., Ohzuku, T. (2004). Systematic Research on Insertion Materials Based on Superlattice Models in a Phase Triangle of LiCoO2 LiNiO2 LiMnO2: I. First-Principles Calculation on Electronic and Crystal Structures, Phase Stability and New Material. Journal of The Electrochemical Society, 151(9): A1499. https://doi.org/10.1149/1.1783908/meta

[4] Yabuuchi, N., Koyama, Y., Nakayama, N., Ohzuku, T. (2005). Solid-State Chemistry and Electrochemistry of LiCo1/ 3Ni1/ 3Mn1/ 3O2 for Advanced Lithium-Ion Batteries: II. Preparation and Characterization. Journal of the Electrochemical Society, 152(7): A1434. https://doi.org/10.1149/1.1924227/meta

[5] Yabuuchi, N., Yoshii, K., Myung, S.T., Nakai, I., Komaba, S. (2011). Detailed studies of a high-capacity electrode material for rechargeable batteries, Li2MnO3− LiCo1/3Ni1/3Mn1/3O2. Journal of the American Chemical Society, 133(12): 4404-4419. https://doi.org/10.1021/ja108588y

[6] Armstrong, A.R., Robertson, A.D., Bruce, P.G. (2005). Overcharging manganese oxides: Extracting lithium beyond Mn4+. Journal of power sources, 146(1-2): 275-280. https://doi.org/10.1016/j.jpowsour.2005.03.104

[7] Guo, X.J., Li, Y.X., Zheng, M., Zheng, J.M., Li, J., Gong, Z.L., Yang, Y. (2008). Structural and electrochemical characterization of xLi [Li1/3Mn2/3] O2·(1− x) Li [Ni1/3Mn1/3Co1/3] O2 (0≤ x≤ 0.9) as cathode materials for lithium ion batteries. Journal of Power Sources, 184(2): 414-419. https://doi.org/10.1016/j.jpowsour.2008.04.013

[8] Li, X., Chen, L., He, W., Peng, F., Xiao, Z. (2014). Hydrothermal synthesis of uniform nanosized lithium-rich cathode material Li0. 94 [Li0. 14Ni0. 26Mn0. 60] O2 for high power lithium-ion batteries. Micro & Nano Letters, 9(1): 19-23. https://doi.org/10.1049/mnl.2013.0613

[9] Yang, S., Huang, G., Hu, S., Hou, X., Huang, Y., Yue, M., Lei, G. (2014). Improved electrochemical performance of the Li1. 2Ni0. 13Co0. 13Mn0. 54O2 wired by CNT networks for lithium-ion batteries. Materials Letters, 118: 8-11. https://doi.org/10.1016/j.matlet.2013.11.071

[10] Thackeray, M.M., Kang, S.H., Johnson, C.S., Vaughey, J.T., Benedek, R., Hackney, S.A. (2007). Li 2 MnO 3-stabilized LiMO 2 (M= Mn, Ni, Co) electrodes for lithium-ion batteries. Journal of Materials chemistry, 17(30): 3112-3125. https://doi.org/10.1039/B702425H

[11] Mohanty, D., Kalnaus, S., Meisner, R.A., Rhodes, K.J., Li, J., Payzant, E.A., Daniel, C. (2013). Structural transformation of a lithium-rich Li1. 2Co0. 1Mn0. 55Ni0. 15O2 cathode during high voltage cycling resolved by in situ X-ray diffraction. Journal of Power Sources, 229: 239-248. https://doi.org/10.1016/j.jpowsour.2012.11.144

[12] Li, Z., Du, F., Bie, X., Zhang, D., Cai, Y., Cui, X., Wei, Y. (2010). Electrochemical kinetics of the Li [Li0. 23Co0. 3Mn0. 47] O2 cathode material studied by GITT and EIS. The Journal of Physical Chemistry C, 114(51): 22751-22757. https://doi.org/10.1021/jp1088788

[13] Shi, S.J., Tu, J.P., Tang, Y.Y., Yu, Y.X., Zhang, Y.Q., Wang, X.L. (2013). Synthesis and electrochemical performance of Li1. 131Mn0. 504Ni0. 243Co0. 122O2 cathode materials for lithium ion batteries via freeze drying. Journal of Power Sources, 221: 300-307. https://doi.org/10.1016/j.jpowsour.2012.08.031

[14] Shi, S.J., Tu, J.P., Tang, Y.Y., Zhang, Y.Q., Wang, X.L., Gu, C.D. (2013). Preparation and characterization of macroporous Li1. 2Mn0. 54Ni0. 13Co0. 13O2 cathode material for lithium-ion batteries via aerogel template. Journal of power sources, 240: 140-148. https://doi.org/10.1016/j.jpowsour.2013.04.006

[15] Lengyel, M., Elhassid, D., Atlas, G., Moller, W.T., Axelbaum, R.L. (2014). Development of a scalable spray pyrolysis process for the production of non-hollow battery materials. Journal of Power Sources, 266: 175-178. https://doi.org/10.1016/j.jpowsour.2014.04.143

[16] Zhao, J., Wang, Z., Guo, H., Li, X., He, Z., & Li, T. (2015). Synthesis and electrochemical characterization of Zn-doped Li-rich layered Li [Li0. 2Mn0. 54Ni0. 13Co0. 13] O2 cathode material. Ceramics International,

41(9): 11396-11401. https://doi.org/10.1016/j.ceramint.2015.05.102

[17] He, Z., Wang, Z., Cheng, L., Zhu, Z., Li, T., Li, X., Guo, H. (2014). Structural and electrochemical characterization of layered 0.3 Li2MnO3· 0.7 LiMn0. 35− x/3Ni0. 5− x/3Co0. 15− x/3CrxO2 cathode synthesized by spray drying. Advanced Powder Technology, 25(2): 647-653. https://doi.org/10.1016/j.apt.2013.10.008

[18] Song, B., Lai, M.O., Lu, L. (2012). Influence of Ru substitution on Li-rich 0.55 Li2MnO3 0.45 LiNi1/3Co1/3Mn1/3O2 cathode for Li-ion batteries. Electrochimica Acta, 80: 187-195. https://doi.org/10.1016/j.electacta.2012.06.118

[19] Wang, D., Huang, Y., Huo, Z., Chen, L. (2013). Synthesize and electrochemical characterization of Mg-doped Li-rich layered Li [Li0. 2Ni0. 2Mn0. 6] O2 cathode material. Electrochimica Acta, 107: 461-466. https://doi.org/10.1016/j.electacta.2013.05.145

[20] Li, Q., Li, G., Fu, C., Luo, D., Fan, J., Li, L. (2014). K+-doped Li1. 2Mn0. 54Co0. 13Ni0. 13O2: a novel cathode material with an enhanced cycling stability for lithium-ion batteries. ACS applied materials & interfaces, 6(13): 10330-10341. https://doi.org/10.1021/am5017649

[21] Du, J., Shan, Z., Zhu, K., Liu, X., Tian, J., Du, H. (2015). Improved electrochemical performance of Li [Li 0.2 Mn 0.54 Ni 0.13 Co 0.13] O 2 by doping with molybdenum for Lithium battery. Journal of Solid State Electrochemistry, 19(4): 1037-1044. https://doi.org/10.1007/s10008-014-2706-6

[22] Du, K., Yang, F., Hu, G.R., Peng, Z.D., Cao, Y.B., Ryu, K.S. (2013). Sodium additive to improve rate performance of Li [Li0. 2Mn0. 54Ni0. 13Co0. 13] O2 material for Li-ion batteries. Journal of power sources, 244: 29-34. https://doi.org/10.1016/j.jpowsour.2013.04.152

[23] Wu, C., Fang, X., Guo, X., Mao, Y., Ma, J., Zhao, C., Chen, L. (2013). Surface modification of Li1. 2Mn0. 54Co0. 13Ni0. 13O2 with conducting polypyrrole. Journal of power sources, 231: 44-49. https://doi.org/10.1016/j.jpowsour.2012.11.138

[24] He, Z., Wang, Z., Guo, H., Li, X., Xianwen, W., Yue, P., Wang, J. (2013). A simple method of preparing graphene-coated Li [Li0. 2Mn0. 54Ni0. 13Co0. 13] O2 for lithium-ion batteries. Materials Letters, 91: 261-264. https://doi.org/10.1016/j.matlet.2012.09.115

[25] Zhang, X., Sun, S., Wu, Q., Wan, N., Pan, D., Bai, Y. (2015). Improved electrochemical and thermal performances of layered Li [Li0. 2Ni0. 17Co0. 07Mn0. 56] O2 via Li2ZrO3 surface modification. Journal of Power Sources, 282: 378-384. https://doi.org/10.1016/j.jpowsour.2015.02.081

[26] Li, Z., Hong, J.H., Gang, H., Lü, L. (2015). Effect of FePO4 coating on performance of Li1. 2Mn0. 54Ni0. 13Co0. 13O2 as cathode material for Li-ion battery. J Inorg Mater, 30(2): 129-134.

[27] Lee, E., Manthiram, A. (2015). High Capacity Li [Li0. 2Mn0. 54Ni0. 13Co0. 13] O2–VO2 (B) Composite Cathodes with Controlled Irreversible Capacity Loss for Lithium-Ion Batteries. Journal of the Electrochemical Society, 158(1): A47-A50.

[28] Na, S.H., Kim, H.S., Moon, S.I. (2005). Synthesis and electrochemical study of Zr-doped LiNixMnyCo (1-x–y) O2 as cathode material for secondary Li-ion battery. In Materials Science Forum, 486: 614-617. https://doi.org/10.4028/www.scientific.net/MSF.486-487.614

[29] Jiang, K.C., Xin, S., Lee, J.S., Kim, J., Xiao, X.L., Guo, Y.G. (2012). Improved kinetics of LiNi 1/3 Mn 1/3 Co 1/3 O 2 cathode material through reduced graphene oxide networks. Physical chemistry chemical physics, 14(8): 2934-2939. https://doi.org/10.1039/C2CP23363K

[30] Zhang, L., Wu, B., Li, N., Mu, D., Zhang, C., Wu, F. (2013). Rod-like hierarchical nano/micro Li1. 2Ni0. 2Mn0. 6O2 as high performance cathode materials for lithium-ion batteries. Journal of power sources, 240: 644-652. https://doi.org/10.1016/j.jpowsour.2013.05.019

[31] Wu, F., Wang, M., Su, Y., Bao, L., Chen, S. (2010). A novel method for synthesis of layered LiNi1/3Mn1/3Co1/3O2 as cathode material for lithium-ion battery. Journal of Power Sources, 195(8): 2362-2367. https://doi.org/10.1016/j.jpowsour.2009.10.043

[32] Oh, S.W., Park, S.H., Park, C.W., Sun, Y.K. (2004). Structural and electrochemical properties of layered Li [Ni0. 5Mn0. 5] 1− xCoxO2 positive materials synthesized by ultrasonic spray pyrolysis method. Solid State Ionics, 171(3-4): 167-172. https://doi.org/10.1016/j.ssi.2004.04.012

[33] Yin, K., Fang, W., Zhong, B., Guo, X., Tang, Y., Nie, X. (2012). The effects of precipitant agent on structure and performance of LiNi1/3Co1/3Mn1/3O2 cathode material via a carbonate co-precipitation method. Electrochimica acta, 85: 99-103. https://doi.org/10.1016/j.electacta.2012.06.064

[34] Ryu, W.H., Lim, S.J., Kim, W.K., Kwon, H. (2014). 3-D dumbbell-like LiNi1/3Mn1/3Co1/3O2 cathode materials assembled with nano-building blocks for lithium-ion batteries. Journal of Power Sources, 257: 186-191. https://doi.org/10.1016/j.jpowsour.2014.02.003